Journal of Naval Architecture and Marine Engineering
December, 2007
DOI: 10.3329/jname.v4i2.992 http://jname.8m.net

COMBINED EFFECT OF CONDUCTION AND VISCOUS DISSIPATION ON MAGNETOHYDRODYNAMIC FREE CONVECTION FLOW ALONG A VERTICAL FLAT PLATE

Abdullah-Al-Mamun[1], Nur Hosain Md. Ariful Azim[2] and Md. Abdul Maleque[3]

[1]Institute of Natural Sciences, United International University, Dhaka-1209, Bangladesh, Email: mamun3213ssh@gmail.com, Phone: 880-2-9125912-5, Fax: 880-2-9125916.
[2]School of Business studies, Southeast University, Banani, Dhaka-1213, Bangladesh, Email: nhmarif@yahoo.com, Phone: 880-2-8860456-7, Ext-229, Fax: 880-2-9892914.
[3] Department of Mathematics, Bangladesh University of Engineering and Technology, Dhaka-1000, Bangladesh.

Abstract

This paper concerns the effects of conduction and viscous dissipation on natural convection flow of an incompressible, viscous and electrically conducting fluid in the presence of transverse magnetic field. Numerical solutions for the governing momentum and energy equations are given. A discussion has been provided for the effects of magnetic parameter, Prandtl number, conjugate conduction parameter and viscous dissipation parameter on two-dimensional flow. Results for the details of the velocity, temperature distributions as well as the skin friction and the rate of heat transfer are shown graphically. Also the numerical values of the surface temperature distributions are presented in tabular form.

Key words: *Viscous dissipation, conduction, convection, magnetohydrodynamics, finite difference method.*

NOMENCLATURE

b	plate thickness	T_f	temperature of the fluid
C_{fx}	local skin friction coefficient	T_s	solid temperature
c_p	specific heat	T_∞	fluid asymptotic temperature
f	dimensionless stream function	$\bar{u}, \bar{v}$	velocity components
g	acceleration due to gravity	u, v	dimensionless velocity components
h	dimensionless temperature	$\bar{x}, \bar{y}$	Cartesian coordinates
H_0	strength of the magnetic field	x,y	dimensionless Cartesian coordinates
K_f, K_s	fluid and solid thermal conductivities, respectively	β	co-efficient of thermal expansion
l	length of the plate	η	dimensionless similarity variable
M	magnetic parameter	θ	dimensionless temperature
N	viscous dissipation parameter	μ, ν	dynamic and kinematic viscosities, respectively
Nu_x	local Nusselt number	ρ	density of the fluid
p	conjugate conduction parameter	σ	electrical conductivity
Pr	Prandtl number	τ_w	shearing stress
q_w	heat flux	ψ	Stream function
T_b	temperature at outside surface of the plate		

1. Introduction

In previous investigations the wall conduction resistance in the case of convective heat transfer between a solid wall and a fluid flow is generally neglected i.e. the wall is assumed to be very thin. But in practical occurrences the neglecting of wall conduction resistance is not possible because of its significant affect in fluid flow and the heat transfer characteristics of the fluid in the vicinity of the wall. In order to take account of physical reality, there has been a proclivity to move away from considering idealized mathematical problems in which the bounding wall is considered to be infinitesimally thin. Thus the conduction in solid wall and the convection in the fluid should be determined simultaneously. This type of convective heat transfer is referred to a conjugate heat transfer (CHT) process and it arises due to the finite thickness of the wall.

The early theoretical and experimental work of CHT problem for a viscous fluid has been reviewed by Gdalevich and Fertman (1977) and Miyamoto et al.(1980). Gdalevich and Fertman (1977) discussed the method, the specifics and the principal results in the previously obtained solutions of conjugate problems of free convection. They stated conclusively that the use of numerical methods for solving the initial system of governing partial differential equations, such as finite difference method, is evidently the most promising in studies of conjugate free convection. Miyamoto et al. (1980) have given an analysis of the relative importance of the parameters of the problem in particular with reference to coaxial heat conduction. Cheng Long Chang (2006) analyzed the conjugate heat transfer of a micropolar fluid for a vertical flat plate. The same problem over a vertical surface in absence of micropolar fluid was studied by Merkin and Pop (1996) and Pozzi and Lupo (1988). Pop et al. (1995) then extended the analysis to conjugate mixed convection on a vertical surface in porous medium. Moreover, the thermal interaction between laminar film condensation and forced convection along a conducting wall was investigated by Chen and Chang (1996). Shu and Pop (1999) analyzed the thermal interaction between free convection and forced convection along a vertical conducting wall. Vynnycky and Kimura (1996) studied numerically the two dimensional conjugate free convection due to a vertical plate of finite extent adjacent to a semi-infinite porous medium using finite difference techniques. Hossain (1992) studied the effect of viscous and Joule heating on the flow of an electrically conducting fluid past a semi infinite plate of which temperature varies linearly with the distance from the leading edge and in the presence of uniformly transverse magnetic field. In his paper, using Keller box (1978) scheme the equations governing the flow were solved and the numerical solutions were obtained for small Prandtl numbers, appropriate for coolant liquid metal, in the presence of a large magnetic field. Amin (2003) investigated the effects of viscous dissipation on buoyancy-induced flow over a horizontal or a vertical flat plate embedded in a Non-Newtonian fluid saturated porous medium under the action of transverse magnetic field. He used the Ostwald-de Waele power-law model to characterize the non-Newtonian fluid behavior. Amin (2003) also analyzed the influences of both first- and second-order resistance, due to the solid matrix of non-darcy porous medium, Joule heating and viscous dissipation on forced convection flow from a horizontal circular cylinder under the action of transverse magnetic field.

To our best knowledge, the effect of magnetic field and viscous dissipation on the coupling of conduction with laminar natural convection along a flat plate has not been studied yet and the present work demonstrates the issue. With a goal to attain similarity solutions of the problem posed, the developed equations are made dimensionless by using suitable transformations. The nondimensional equations are then transformed into non-linear equations by introducing a non- similarity transformation. The resulting non-linear equations together with their corresponding boundary conditions based on conduction and convection are solved numerically by using the finite difference method along with Newton's linearization approximation. Here we have focused our attention on the evolution of the surface shear stress in terms of local skin friction and the rate of heat transfer in terms of local Nusselt number, velocity profiles as well as temperature profiles for different values of the parameters entering into the problem.

2. Mathematical Model

Let us consider a steady free convection flow of an electrically conducting, viscous and incompressible fluid adjacent to a vertical flat plate of length l and thickness b of ambient temperature T_∞ (Fig. 1). It is assumed that heat is transferred from the outside surface of the plate, which is maintained at the constant temperature T_b where $T_b > T_\infty$. A uniform magnetic field of strength H_0 is imposed along the $\bar{y}$ -axis.

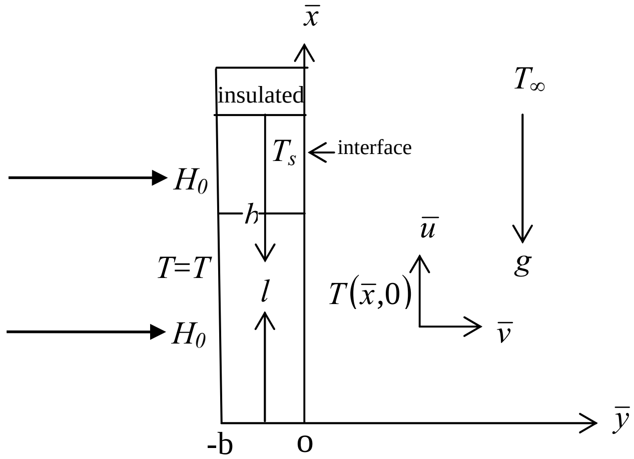

Fig.1: Physical model and coordinate system.

The energy equation in the solid plate is given by

$$\frac{\partial^2 T_s}{\partial \bar{x}^2} + \frac{\partial^2 T_s}{\partial \bar{y}^2} = 0 \quad \text{for} \quad 0 \le \bar{x} \le l, \quad -b \le \bar{y} \le 0 \tag{1}$$

and this equation is coupled to the energy equation in the fluid region by the condition that the temperature and the heat flux are continuous at the solid-fluid interface, namely

$$T_s = T_f \quad \text{on} \quad \bar{y} = 0, \quad 0 \le \bar{x} \le l \tag{2}$$

$$k_s \frac{\partial T_s}{\partial \bar{y}} = k_f \frac{\partial T_f}{\partial \bar{y}} \quad \text{on} \quad \bar{y} = 0, \quad 0 \le \bar{x} \le l, \tag{3}$$

where T_s and T_f are the temperatures of the solid and fluid respectively and K_s and K_f are thermal conductivities of the solid and fluid respectively.

Generally the axial heat conduction along the wall is negligible when compared with the normal conduction across the wall and this assumption is consistent with the boundary layer theory (1974, 1996). Thus equation (1) reduces to

$$\frac{\partial^2 T_s}{\partial \bar{y}^2} = 0 \quad \text{for} \quad 0 \le \bar{x} \le l, \quad -b \le \bar{y} \le 0 \tag{4}$$

But the assumption of the neglection of the axial conduction of heat from equation (1) is only valid provided that the ratio of the wall thickness to the length of the plate is small. i.e. $b / l << 1$. Therefore applying the condition that $T_s = T_b$ on $y = -b$ in equation (1) we get

$$T_s(\bar{x}, \bar{y}) = T(\bar{x}, 0) + \{T(\bar{x}, 0) - T_b\} \bar{y} / b \tag{5}$$

where $T(\bar{x},0)$ is the unknown temperature at the solid-fluid interface and this is determined by the solution of the governing equations. Thus the condition (3) can be written as follows

$$T(\bar{x}, o) - T_b = (k_f / k_s) b \left(\frac{\partial T_f}{\partial \bar{y}} \right)_{\bar{y}=0} \tag{6}$$

Thus the boundary layer equations governing the convective flow under these assumptions with the Boussinesq approximations can be written as

$$\frac{\partial \bar{u}}{\partial \bar{x}}+\frac{\partial \bar{v}}{\partial \bar{y}}=0 \tag{7}$$

$$\bar{u}\frac{\partial \bar{u}}{\partial \bar{x}}+\bar{v}\frac{\partial \bar{u}}{\partial \bar{y}}=\nu\frac{\partial^2 \bar{u}}{\partial \bar{y}^2}+g\beta(T_f-T_\infty)-\frac{\sigma H_0{}^2\bar{u}}{\rho} \tag{8}$$

$$\bar{u}\frac{\partial T}{\partial \bar{x}}+\bar{v}\frac{\partial T}{\partial \bar{y}}=\frac{k_f}{\rho c_p}\frac{\partial^2 T}{\partial \bar{y}^2}+\frac{\nu}{c_p}\left(\frac{\partial \bar{u}}{\partial \bar{y}}\right)^2 \tag{9}$$

which have to be solved along with the following boundary conditions:

$$\left.\begin{array}{l}\bar{u}=0,\bar{v}=0\\ T_f=T(\bar{x},0),\ \dfrac{\partial T_f}{\partial \bar{y}}=\dfrac{k_s}{b k_f}\left(T_f-T_b\right)\end{array}\right\}\text{on } \bar{y}=0,\ \bar{x}>0 \tag{10}$$

$$\bar{u}\to 0, T_f\to T_\infty \text{ as } \bar{y}\to\infty,\ \ \bar{x}>0$$

Introducing the following nondimensional quantities:

$$x=\frac{\bar{x}}{l},\ y=\frac{\bar{y}}{l}Gr^{\frac{1}{4}},\ u=\frac{\bar{u}l}{\nu}Gr^{-\frac{1}{2}},\ v=\frac{\bar{v}l}{\nu}Gr^{-\frac{1}{4}},\ \frac{T-T_\infty}{T_b-T_\infty}=\theta,$$
$$Gr=g\beta l^3\left(T_b-T_\infty\right)/\nu^2 \tag{11}$$

where l is the length of the plate, Gr is the Grashof number and θ is the non-dimensional temperature, the governing equations are obtained in the following non dimensional form:

$$\frac{\partial u}{\partial x}+\frac{\partial v}{\partial y}=0 \tag{12}$$

$$u\frac{\partial u}{\partial x}+v\frac{\partial u}{\partial y}+Mu=\frac{\partial^2 u}{\partial y^2}+\theta \tag{13}$$

$$u\frac{\partial \theta}{\partial x}+v\frac{\partial \theta}{\partial y}=\frac{1}{\Pr}\frac{\partial^2 \theta}{\partial y^2}+N\left(\frac{\partial u}{\partial y}\right)^2 \tag{14}$$

where $\Pr=\dfrac{\mu c_p}{k}$ is the prandtl number, $M=\sigma H_0^2 l^2/\mu Gr^{1/2}$ is the magnetic parameter and $N=\nu^2 Gr/l^2 c_p\left(T_b-T_\infty\right)$ is the viscous dissipation parameter

The corresponding boundary conditions in a non dimensional form are given by

$$u=v=0,\ \theta-1=p\frac{\partial \theta}{\partial y} \quad \text{on} \quad y=0,\ x>0$$
$$u\to 0,\ \theta\to 0 \quad \text{as} \quad y\to\infty,\ x>0 \tag{15}$$

where $p=\left(k_f/k_s\right)\left(b/l\right)Gr^{1/4}$ is the conjugate conduction parameter.

To solve the equations (13) and (14) subject to the boundary conditions (15), we assume the following variables

$$\psi=x^{4/5}\left(1+x\right)^{-1/20}f\left(x,\eta\right),\ \eta=yx^{-1/5}\left(1+x\right)^{-1/20},\ \theta=x^{1/5}\left(1+x\right)^{-1/5}h\left(x,\eta\right) \tag{16}$$

Here η is the similarity variable and ψ is the non-dimensional stream function which satisfies the equation of continuity and which is related to the velocity components in the usual way as $u = \partial\psi/\partial y, v = -\partial\psi/\partial x$ and $h(x,\eta)$ is the dimensionless temperature.

It may be continued to transform the momentum and energy equations (13) and (14) respectively into the new co-ordinate systems. In order to make easy the transformation, it is useful to enclose the velocity components unambiguously expressed in terms of the new variables. Hence we get

$$f''' + \frac{16+15x}{20(1+x)} ff'' - \frac{6+5x}{10(1+x)} f'^2 - Mx^{2/5}(1+x)^{1/10} f' + h = x\left(f' \frac{\partial f'}{\partial x} - f'' \frac{\partial f}{\partial x} \right) \tag{17}$$

$$\frac{1}{\Pr} h'' + \frac{16+15x}{20(1+x)} fh' - \frac{1}{5(1+x)} f'h + Nxf''^2 = x\left(f' \frac{\partial h}{\partial x} - h' \frac{\partial f}{\partial x} \right) \tag{18}$$

where primes denote differentiation with respect to η .

The boundary conditions (15) then take the following form

$$f(x,0) = f'(x,0) = 0, \; ph'(x,0) = -(1+x)^{1/4} + x^{1/5}(1+x)^{1/20} h(x,0)$$
$$f'(x,\infty) \to 0, \; h(x,\infty) \to 0 \tag{19}$$

The set of equations (17) and (18) together with the boundary conditions (19) are solved numerically by applying implicit finite difference method with Keller box [11] scheme. Since a good description of this method and its application to the boundary layer flow problems are given in the book by Cebeci and Bradshaw [17], the details of the method have not been presented in this paper. From the process of numerical computation, in practical point of view, it is important to calculate the values of the rate of heat transfer and surface shear stress in terms of Nusselt number and the skin friction coefficient respectively. These can be written in the non-dimensional form as

$$C_f = \frac{Gr^{-3/4} l^2}{\mu \nu} \tau_w \quad \text{and} \quad Nu = \frac{l Gr^{-1/4}}{k_f (T_b - T_\infty)} q_w \tag{20}$$

where $\tau_w = \mu \left(\frac{\partial \bar{u}}{\partial \bar{y}} \right)_{\bar{y}=0}$ and $q_w = -k_f \left(\frac{\partial T_f}{\partial \bar{y}} \right)_{\bar{y}=0}$, K_f being the thermal conductivity of the fluid.

Using the new variables described in (12), we have

$$C_{fx} = x^{2/5}(1+x)^{-3/20} f''(x,0) \tag{21}$$

$$Nu_x = -(1+x)^{-1/4} h'(x,0) \tag{22}$$

Also the numerical values of the surface temperature distribution are obtained from the relation

$$\theta(x,0) = x^{1/5}(1+x)^{-1/5} h(x,0) \tag{23}$$

and for different values of the Prandtl number *Pr* and the conduction parameter *p*, the surface temperature distribution are displayed in tabular form.

Moreover, we have discussed the velocity profiles and the temperature distributions for different values of magnetic parameter *M*, the viscous dissipation parameter *N*, the conjugate conduction parameter *p* and the Prandtl number *Pr*.

5. Results and Discussion

The resulting solutions for the velocity and temperature functions are shown graphically in Figs. 2, 3, 4 and 5. The values of Prandtl numbers are taken to be 1.74, 1.0, 0.90 and 0.733 which correspond to water, stem, ammonia and air, respectively. In fact, detailed numerical solutions have been obtained for a wide range of values of the viscous dissipation parameter N (= 1.0, 0.5, 0.2, 0.08, 0.05, 0.01), magnetic parameter M (= 1.0, 0.8, 0.5, 0.2) and conjugate conduction parameter p (= 1.0, 2.0, 2.5, 3.0).

A comparison of the surface temperature and the local skin friction factor obtained in the present work with $x^{1/5} = \xi$, M = 0, N = 0, and p = 1.0 and obtained by Pozzi and Lupo and Merkin and Pop (2001) have been shown in Table 1 and Table 2, respectively. It is clearly seen that there is an excellent agreement among the respective results.

Table 1: Comparison of the present numerical results of surface temperature with Prandtl number Pr = 0.733 and M = 0, N = 0 and p = 1.0.

	$\theta(x,0)$		
$x^{1/5} = \xi$	Pozzi and Lupo (1988)	Merkin and Pop (1996)	Present work
0.7	0.651	0.651	0.651
0.8	0.684	0.686	0.687
0.9	0.708	0.715	0.716
1.0	0.717	0.741	0.741
1.1	0.699	0.762	0.763
1.2	0.640	0.781	0.781

Table 2: Comparison of the present numerical results of skin friction coefficient with Prandtl number Pr = 0.733 and M = 0, N = 0 and p=1.

	C_{fx}		
$x^{1/5} = \xi$	Pozzi and Lupo (1988)	Merkin and Pop (1996)	Present work
0.7	0.430	0.430	0.424
0.8	0.530	0.530	0.529
0.9	0.635	0.635	0.635
1.0	0.741	0.745	0.744
1.1	0.829	0.859	0.860
1.2	0.817	0.972	0.975

Figures 2(a) and (b) illustrate the behavior of the velocity and the temperature profiles for different values of M with Pr = 0.733, p = 2.5 and N = 0.01. From Fig. 2(a), we may conclude that for increasing values in M; the Lorentz force, which opposes the flow, there is a fall in velocity maximum due to the retarding effect of the magnetic force in the region $\eta \in [0, 10]$. As a result the momentum boundary layer thickness becomes larger and the separation of the boundary layer will occur earlier. An opposite situation is observed from Fig. 2(b) in the case of temperature field. It implies that the magnetic field works to increase the values of the temperature in the flow region and then decreases the gradient at the wall and increases the thickness of the thermal boundary layer. Figures 3(a) and (b) represent the velocity and the temperature field, respectively for different values of Pr with M = 0.5, N = 0.01 and p = 2.5. Both velocity and temperature decrease as Pr increases. This is an agreement with the physical fact that the thermal boundary layer thickness decreases with increasing *Pr*. Figures 4(a) and (b) depict the velocity and temperature profiles for different values of *p* in presence of magnetic field with viscous dissipation while *Pr* = 0.733. From Fig. 4(a), we may conclude that the velocity profile is influenced significantly and decreases when the value of *p* increases. But it is seen that near the surface of the flat plate the velocity increases by a long way and become maximum and then decreases slowly and finally approaches zero. The maximum values of the velocity are 0.3017, 0.3175, 0.3360 and 0.3865 for *p* = 3.0, 2.5, 2.0, 1.0, respectively which occur at η = 1.4975 for the first maximum value, η = 1.4741 for the second maximum value, η = 1.4508 for the third maximum value and at η = 1.3938 for the last maximum value. Here it is found that the velocity profiles decrease by 21.94% while *p* increases from 1.0 to 3.0. On the other hand, in the case of temperature field, from Fig. 4(b), it can be observed that the temperature distribution over the whole boundary layer decreases when the values of the *p* increases. Here it is seen that the maximum values of the temperature profiles are 0.8762, 0.7187, 0.6624 and 0.6157 for *p* = 1.0, 2.0, 2.5 and 3.0, respectively and each of which attains at the surface of the plate. Thus in this case temperature profiles decrease by 29.73% while *p* changes from 1.0 to 3.0. Figures 5(a) and (b) give a picture of velocity and temperature profiles for different values of *N*. We observe from Fig. 5(a) that an increase in the viscous dissipation parameter, *N*, is associated with a slight increase in velocity and a similar situation is observed from Fig. 5(b) in case of temperature field.

The variation of reduced local skin friction coefficient C_{fx} and local rate of heat transfer Nu_x with *Pr* =0.733, *N* = 0.01 and *p* = 2.5 for different values of *M* at different position of *x* are illustrated in Figs. 6(a) and 6(b), respectively. From Fig. 6(a), it can be seen that the magnetic parameter *M* shrinks the wall shear stress. This means that the magnetic force retard the flow and work with the adverse pressure to resist the flow. From Fig. 6(b) it is observed that the local heat transfer rate decreases with increasing *M*. This is because the magnetic force works against the inertia force and as a result the values of the rate of heat transfer reduce. Figures 7(a) and (b) show the local skin friction coefficient and the rate of heat transfer, respectively with respect to the axial distance *x* for different values of *Pr* in presence of magnetic field with viscous dissipation while *p* =2.5. From Fig. 7(a) it can be seen that an increase in the *Pr* is associated with a decrease in the skin friction and an opposite result is observed in the case of rate of heat transfer from Fig. 7(b). Figures 8(a) and (b) represent the skin friction coefficient and the rate heat transfer for different values of *p* with *M* = 0.5, *N* = 0.01 and *Pr* = 0.733. It can be seen; from these two figures that, an increase in the conjugate conduction parameter *p* decreases both skin friction coefficient and the rate of heat transfer. Figures 9(a) and (b) deal with the effect of viscous dissipation parameter on the skin friction coefficient and the rate of heat transfer, respectively against *x* with *M* = 0.5, *p* = 2.5 and *Pr* = 0.733. Fig 9(a) shows that an increase with the viscous dissipation parameter, *N*, is associated with an increase in skin friction and from Fig. 9(b) it is seen that an increase in the parameter *N* is associated with a decrease in the rate of heat transfer.

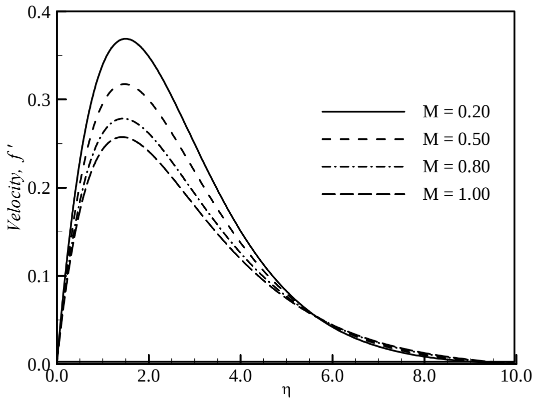

(a)

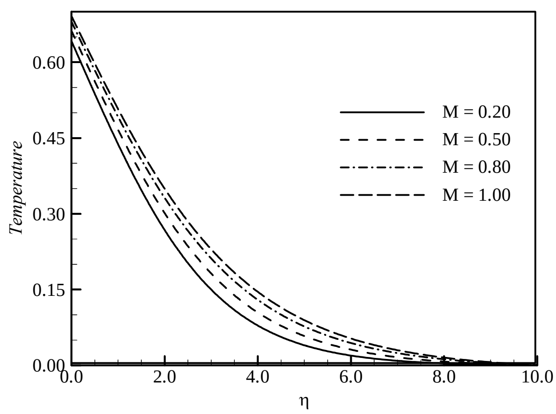

(b)

Fig. 2(a) Variation of velocity profiles and (b) variation of temperature profiles against η for varying of with *Pr* =0.733, *p* = 2.5 and *N* = 0.01.

Numerical values of the surface temperature distribution for different values of *Pr* with *N* = 0.01, *M* = 0.5 and *p* = 2.5 are depicted in Table 3. From Table 3, we found that the values of the surface temperature distribution decrease at different position of *x* for Prandtl number *Pr* = 0.733, 0.90, 1.0 and 1.74. Near the axial position *x* = 3.0, the rate of decrease of the surface temperature distribution is 10.44% as *Pr* changes from 0.733 to 1.74. Furthermore, it is clear from Table 4 that the numerical values of the surface temperature distribution decrease for increasing values of the conjugate conduction parameter *p* and at the same axial position *x* = 3.0049, the rate of decrease of surface temperature distribution is 24.975% as the *p* changes from 1.0 to 3.0.

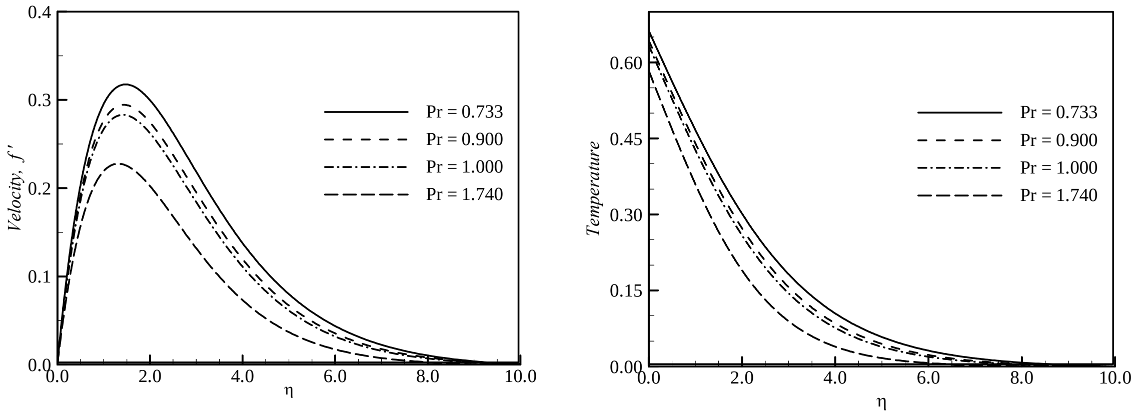

(a) (b)

Fig. 3(a). Variation of velocity profiles and (b) variation of temperature profiles against η for varying of *Pr* with *N* = 0.01, *M* = 0.5 and *p* = 2.5

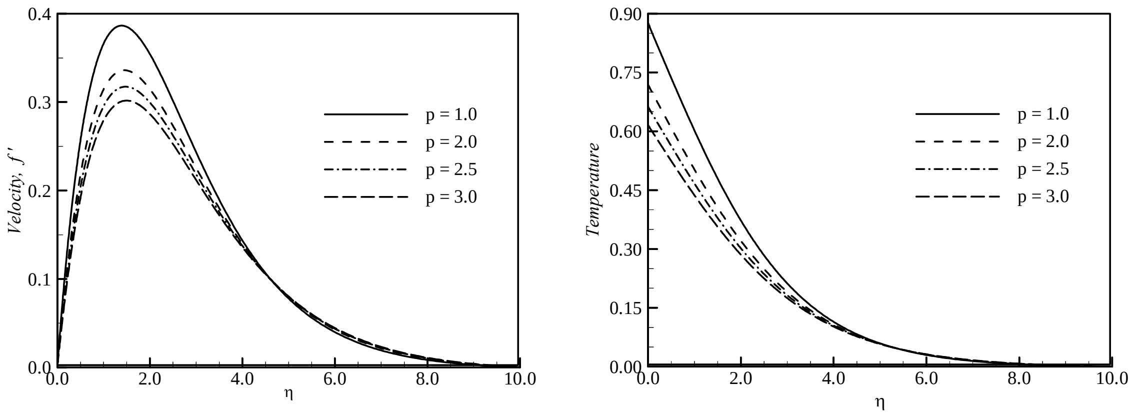

(a) (b)

Fig. 4. (a) Variation of velocity profiles and (b) variation of temperature profiles against η for varying of *p* with *N* = 0.01, *M* = 0.5 and Pr = 0.733

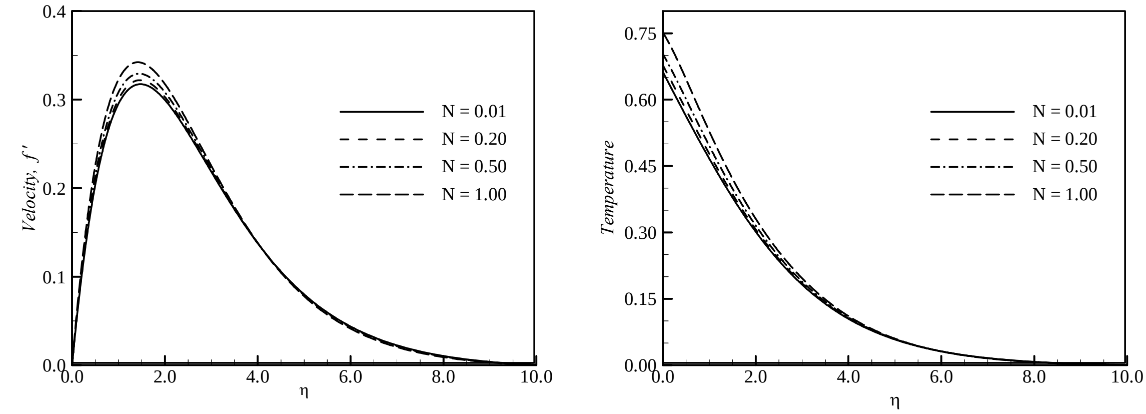

(a) (b)

Fig. 5. (a) Variation of velocity profiles and (b) variation of temperature profiles against η for varying of *N* with *M* = 0.5, *Pr* = 0.733 and *p* = 2.5

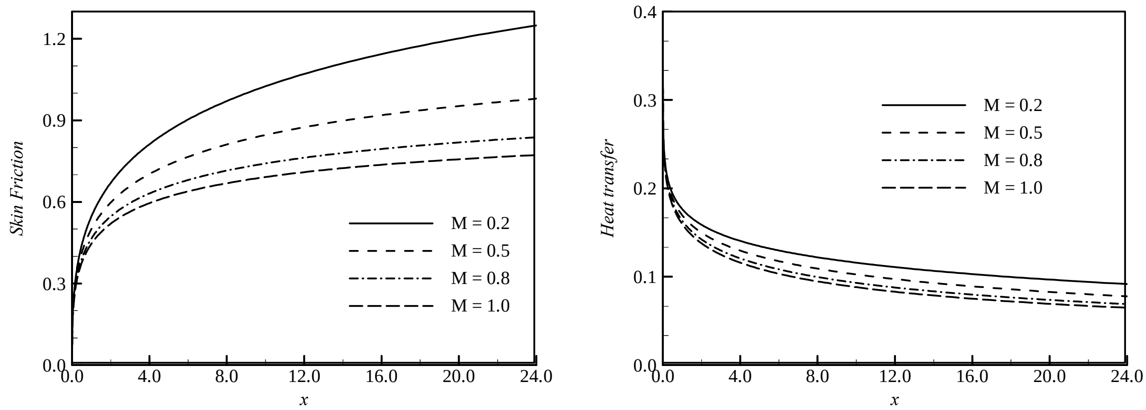

(a) (b)

Fig. 6. (a) Variation of skin friction coefficients and (b) variation of rate of heat transfer against *x* for varying of *M* with *Pr* = 0.733, *N* = 0.01 and *p* = 2.5

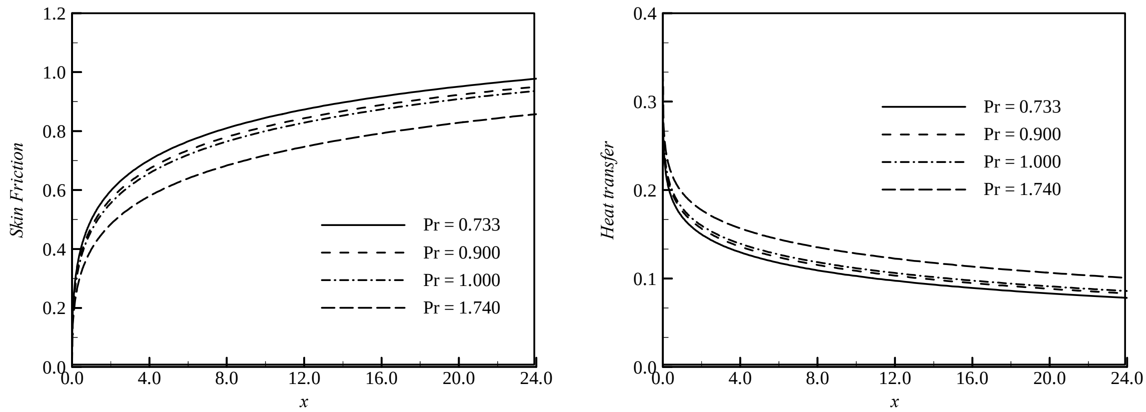

(a) (b)

Fig. 7. (a)Variation of skin friction coefficients and (b) variation of rate of heat transfer against *x* for varying of *Pr* with *M* = 0.5, *N* = 0.01 and *p* = 2.5.

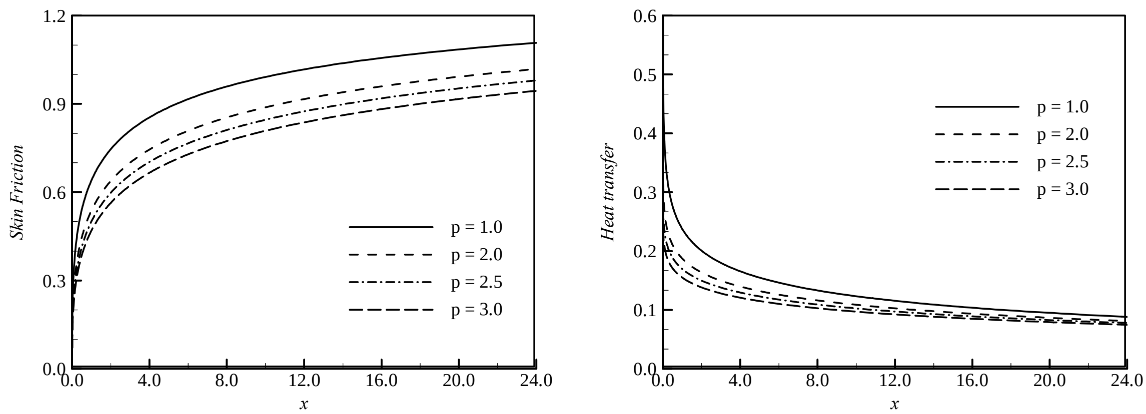

(a) (b)

Fig. 8. (a)Variation of skin friction coefficients and (b) variation of rate of heat transfer against x for varying of p with M = 0.5, N = 0.01 and Pr = 0.733.

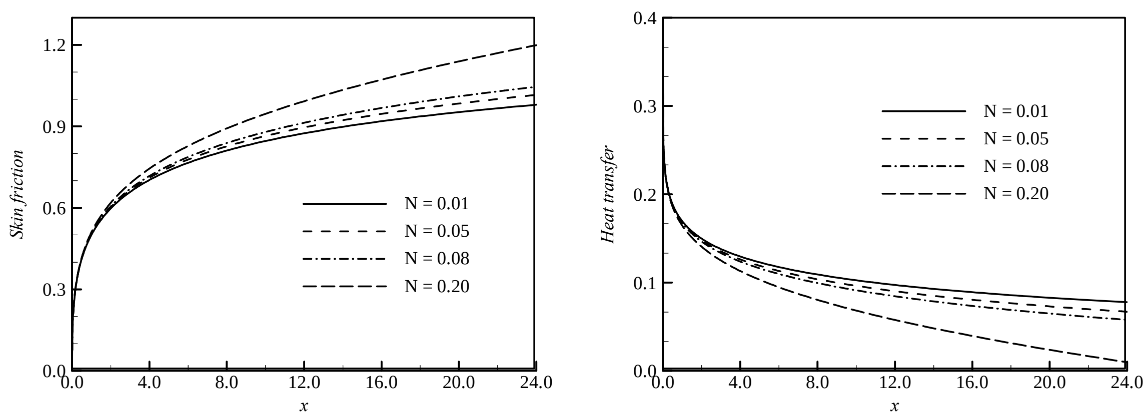

(a) (b)

Fig. 9. (a)Variation of skin friction coefficients and (b) variation of rate of heat transfer against x for varying of N with M = 0.5, Pr = 0.733 and p = 2.5.

Table 3: Numerical values of surface temperature distribution against x for different values of Pr while M=0.5, N = 0.01 and p = 2.5.

x	Pr = 0.733	Pr = 0.90	Pr = 1.0	Pr= 1.74
	$\theta(x,0)$	$\theta(x,0)$	$\theta(x,0)$	$\theta(x,0)$
0.0001	0.1406	0.1335	0.1301	0.1137
0.5211	0.5310	0.5143	0.5059	0.4633
1.0265	0.5777	0.5609	0.5525	0.5090
1.5095	0.6051	0.5884	0.5800	0.5362
2.0369	0.6267	0.6101	0.6017	0.5578
3.0049	0.6551	0.6388	0.6305	0.5867
4.0219	0.6766	0.6605	0.6523	0.6087
5.0387	0.6932	0.6774	0.6693	0.6260

6.0502	0.7067	0.6911	0.6831	0.6402
7.1132	0.7186	0.7033	0.6954	0.6528
8.0285	0.7275	0.7123	0.7045	0.6623

Table 4: Numerical values of surface temperature distribution against x for different values of p while M=0.5, N = 0.01 and Pr = 0.733.

x	p=1.0	p=2.0	p=2.5	p=3.0
	$\theta(x,0)$	$\theta(x,0)$	$\theta(x,0)$	$\theta(x,0)$
0.0001	0.2605	0.1647	0.1406	0.1233
0.5211	0.7285	0.5814	0.5311	0.4901
1.0265	0.7654	0.6272	0.5778	0.5369
1.5095	0.7859	0.6536	0.6053	0.5647
2.0369	0.8015	0.6743	0.6269	0.5868
3.0049	0.8212	0.7011	0.6553	0.6161
4.0219	0.8356	0.7213	0.6768	0.6385
5.0387	0.8464	0.7367	0.6935	0.6559
6.0502	0.8550	0.7492	0.7070	0.6702
7.1132	0.8625	0.7602	0.7190	0.6828
8.0285	0.8679	0.7684	0.7279	0.6922

6. Conclusion

An MHD natural convection flow along a vertical flat plate of thickness b is investigated in the presence of viscous dissipation. The equations governing such flow are transformed to dimensionless form with the help of apposite transformations. The ultimate resulting equations obtained by using the stream function with similarity variable are solved numerically by means of finite difference method with Keller box scheme. The results are shown graphically for different values of the parameters considered in the analysis. The present investigation can be concluded as follows:

1. The velocity of the fluid within the boundary layer decreases with the increasing magnetic parameter, Prandtl number and conjugate conduction parameter while it increases slightly for the increasing viscous dissipation parameter.
2. The temperature of the fluid near the interface increases for the increasing magnetic parameter and dissipation parameter while it decreases for the increasing Prandtl number and conjugate conduction parameter.
3. The shear stress coefficient at the interface increases for the decreasing magnetic parameter, the Prandtl number and conjugate conduction parameter and the increasing dissipation parameter.
4. The rate of heat transfer from the plate to the surface increases for the decreasing magnetic parameter, conjugate conduction parameter, dissipation parameter and the increasing Prandtl number.

References

Chen H.T and Chang S.M., (1996): The Thermal Interaction between Laminar Film Condensation and Forced Convection along a Conducting Wall, Acta Mechanica 118, 13-26. doi:10.1007/BF01410504

Cheng Long Chang,(2006): A Numerical Simulation of Micro Polar Fluid Flow Along a Flat Plate With Wall Conduction And Buoyancy Effects, J. Appl. Phys. D 39,1132-1140. doi:10.1088/0022-3727/39/6/019

El-Amin, M. F. (2003): Combined Effect of Magnetic Field and Viscous Dissipation on a Power-Law Fluid Over Plate With Variable Surface Heat Flux Embedded in a Porous Medium, Journal of Magnetism and Magnetic Materials 261 228-237. doi:10.1016/S0304-8853(02)01478-6

El-Amin, M. F. (2003): Combined Effect of Viscous Dissipation and Joule Heating on MHD Forced Convection Over a Non Isothermal Horizontal Cylinder Embedded in a Fluid Saturated Porous Medium, Journal of Magnetism and Magnetic Materials 263 337-343. doi:10.1016/S0304-8853(03)00109-4

Gdalevich, L. B. and. Fertman, V.E. (1977): Conjugate Problems of Natural Convection, Inzh-Fiz. Zh. 33 (3), 539-547.

Hossain, M. A. (1992): Viscous and Joule Heating Effects on MHD-Free Convection Flow With Variable Plate Temperature, Int. J. Heat Mass Transfer 35, No. 12, pp. 3485-3487. doi:10.1016/0017-9310(92)90234-J

Keller, H. B. (1978): Numerical Methods in The Boundary Layer Theory, Annual Rev. Fluid Mechanics, 10, pp. 417—433. doi:10.1146/annurev.fl.10.010178.002221

Luikob, A. V., Aleksashenko, V. A. and Aleksashenko, A. A. (1971): Analytical Methods of Solution of Conjugated Problems in Convective Heat Transfer, Int. J. Heat Mass Transfer 14, 1047-1056. doi:10.1016/0017-9310(71)90203-1

Merkin, J. H. and Pop, I. (1996): Conjugate Free Convection on a Vertical Surface, Int. Journal of Heat and Mass Transfer 39, 1527-1534. doi:10.1016/0017-9310(95)00238-3

Miyamoto, M. Sumikawa, J. Akiyoshi T. and Nakamura, T. (1980): Effects of Axial Heat Conduction in a Vertical Flat Plate on Free Convection Heat Transfer, Int. J. Heat Mass Transfer 23, 1545-1553. doi:10.1016/0017-9310(80)90158-1

Pop, I. and Ingham, D. B. (2001): Convective Heat Transfer: Mathematical and Computational Modeling of Viscous Fluids and Porous Media (Pergamon, Oxford) p 179.
Pop, I. Lesnic, D. and Ingham, D. B. (1995): Conjugate mixed convection on a vertical surface in a porous medium, Int. J. Heat Mass Transfer 38, 1517-1525. doi:10.1016/0017-9310(94)00340-2

Pozzi, A. and Lupo, M. (1988): The Coupling of Conduction With Laminar Natural Convection Along a Flat Plate, International Journal of Heat and Mass Transferf 31, 1807—1814. doi:10.1016/0017-9310(88)90195-0

Shu, J.J. and Pop, I. (1999): The Thermal Interaction Between Free Convection and Forced Convection Along A Vertical Conducting Wall, International Journal of Heat and Mass Transfer 35, 33-38. doi:10.1007/s002310050295

Vynnycky, M. and Kimura, S. (1996): Transient Conjugate Free Convection Due to a Heated Vertical Plate, Int. J. Heat Mass Transfer 39, 1067-1080. doi:10.1016/0017-9310(95)00188-3